Experimental Investigation and Numerical Simulation of Spray Processes

Julian Laackmann,[*1] *Winfried Säckel,*[*2] *Lina Cepelyte,*[1] *Kamil Walag,*[1] *Robert Sedelmayer,*[1] *Franz Keller,*[2] *Werner Pauer,*[1] *Hans-Ulrich Moritz,*[1] *Ulrich Nieken*[2]

Summary: Acoustic levitation was investigated as a model for spray processes. The influence of different parameters on the drying process of aqueous polyvinylpyrrolidone (PVP) solutions was studied and compared to the evaporation of water. The adequacy of acoustic levitation as model for spray processes was demonstrated. Experiments with water and aqueous PVP solutions indicated no dependency of the droplet size on the drying process for droplets with a diameter between 300 μm and 1.5 mm. Particles dried in an acoustic levitator displayed good accordance of morphology with those obtained in a spray tower. Surprisingly the addition of PVP to water resulted in faster evaporation of the solvent. Mathematical models of single droplets within a spray process typically refer to spherically symmetric droplet geometries. The simulation of other morphologies and their evolution throughout the process is still very challenging. A new drying model based on a fully three-dimensional meshfree approach is under development and shows good agreement to basic established models regarding the drying of a single droplet.

Keywords: acoustic levitation; meshfree simulation; morphology; spray processes; water-soluble polymers

Introduction

Spray processes are widely used in industry. Almost every detergent, instant coffee, milk, egg and tomato powder as well as many chemical, pharmaceutical and biochemical precursors are spray-dried.[1] Depending on the application of the powders, characteristics like free flowing property and the ability to develop enough linkage force between particles for direct compression of tablets are essential. These characteristics are defined by morphological properties which in turn can be influenced by process parameters like temperature, gas flow velocity and droplet size.

Properties of used and obtained substances can be measured, but especially the occurrences during the falling period of the sprayed substances are essential for the understanding of the drying processes. Due to the falling velocity of droplets inside the spray apparatus, observation is difficult. To gain insight into these processes a contactless positioning of the probe material seems to be helpful.

Thus acoustic levitation was investigated as a method for contactless positioning of objects. Using the pressure distribution inside a standing acoustic wave it is possible to levitate solid as well as liquid samples. The relative movement of droplets during the fall in a spray tower can be simulated by generating a gas flow around levitated droplets. Convective mass and heat transfer are taken into account and are comparable to those of a falling droplet.

[1] Institute for Technical and Macromolecular Chemistry, University of Hamburg, Bundesstr. 45, 20146 Hamburg, Germany
Fax: (+49) 40 42838 6008;
E-mail: julian.laackmann@chemie.uni-hamburg.de
[2] Institute of Chemical Process Engineering, University of Stuttgart, Böblinger Str. 78, 70199 Stuttgart, Germany
Fax: (+49) 40 42838 6008;
E-mail: winfried.saeckel@icvt.uni-stuttgart.de

Principle of Acoustic Levitation

First studies regarding the containerless positioning of objects by acoustic forces were published by King in 1934.[2] In the 1970 s the National Aeronautics and Space Administration (NASA) as well as the European Space Agency (ESA) conducted research on acoustic levitation to carry out experiments under microgravity conditions.[3,4] Since then acoustic levitation was subject of many investigations and the principles are well described in literature.[5,6]

The employed acoustic levitator consists of a transducer which oscillates with a frequency in ultra sonic range and a reflector which reflects the generated wave. Due to the identical wavelengths of incoming and reflected waves, it is possible to realize a standing wave by adjusting the transducer and reflector distance. Depending on the distance between transducer and reflector more than one pressure node can be produced. At a distance d of a multiple of a half wavelength λ the resonance condition is given and a stable levitation can be achieved (Eq. (1)).

$$d = n\frac{\lambda}{2} \text{ with } n = 1, 2, 3... \tag{1}$$

The pressure distribution inside the standing wave allows radial as well as axial positioning of small samples and is not dependent on physical properties like electric conductivity or diamagnetism. The standing wave is described by different variables with sound pressure p and particle velocity v being the most important. Sound pressure p results from periodic compression and relaxation of the fluid in the acoustic levitation field (ALF) and is responsible for axial positioning. Equation (2) describes the periodicity of the sound pressure with wave number k and distance z between a pressure node and the transducer.

$$p = p_{\max}\cos(kz) \tag{2}$$

The Bernoulli principle states that an increase in speed is accompanied by a decrease in pressure. Particles in the standing wave oscillate around a virtual idle state where their maximum speed is at the position of the idle state and their minimal speed at the reversal point. Therefore the pressure is highest at the boundaries of the standing wave and decreases towards the levitation axis. This results in a radial positioning of objects in the ALF and is described by Eq. (3).

$$v = v_{\max}\sin(kz) \tag{3}$$

Combination of the effects of axial and radial positioning forces compensates gravitational forces and allows levitation of objects. On earth levitation occurs slightly beneath the pressure node due to gravitaty (Figure 1).

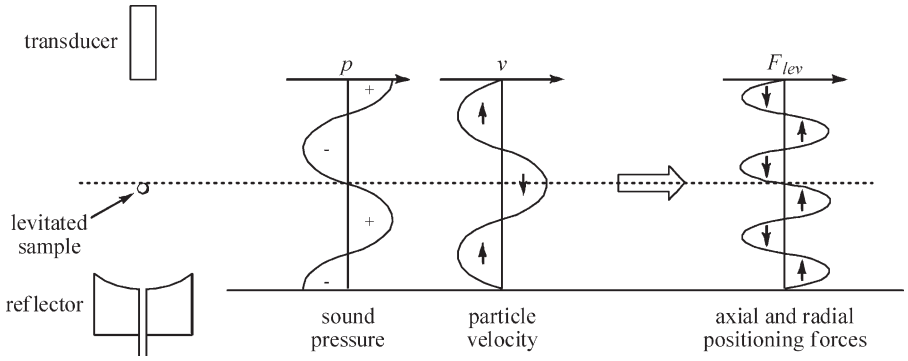

Figure 1.
Sound pressure and particle velocity in a standing acoustic wave between transducer and reflector of an acoustic levitator.

Experimental Part

All experiments were conducted with a non-commercial acoustic levitator working at 42 kHz. Temperatures above room temperature (rt) were generated by employing a process chamber which was positioned around the ALF. On the outer surface of the chamber a resistance wire was attached and the setup was isolated with glass wool. The used reflectors were punctuated with one respectively five vents in the centre as inlet for a gas flow around the levitated droplets.

Aqueous solutions of polyvinylpyrrolidone (PVP) were prepared by dissolving Kollidon® 30 (BASF SE, Germany) in bidestilled water. All reference experiments were performed with bidestilled water.

There were in principle two different methods for the insertion of droplets with a diameter up to 2.5 mm into the ALF. The solution was either nebulized by the transducer, the resulting mist then accumulates in split second in all pressure nodes, or the solution was inserted directly into one specific pressure node with a capillary.

The inserted droplets were observed with a camera (PixeLINK PL-A741) in front of an illuminated background. The recorded images were analyzed with the software ProAnalyst which gave the cross sectional area in pixel. The conversion into SI units was carried out via a calibration with a microscope scale.

The scanning electron microscope (SEM) LEO 1525 was used to investigate the morphology of dried particles.

Spray drying experiments were conducted in a tower with a height of 14 m. Solutions were introduced into the tower with a self constructed droplet generator which yields a droplet chain through an aperture. The droplets were up to 300 μm in diameter. The temperature was controlled with a heated parallel gas flow and the temperature decreased from 225 °C at the intake to 90 °C at the outlet.

Single Droplet Drying in an Acoustic Levitator

In this section the drying kinetics of aqueous PVP solutions are discussed. The influence of process parameters like temperature, droplet size, gas flow and concentration on the drying process are investigated to study the transferability of the results to actual conditions in a spray process and to demonstrate the reproducibility of experiments in the acoustic levitator.

Influence of the Temperature on Drying Kinetics

During the drying energy for the phase transition of the solvent into the gaseous phase is taken from the vicinity. Hence the temperature of the drying solution is lower than the temperature of the surrounding medium. By raising the gas atmosphere temperature the evaporation proceeds faster, because the system is provided with more energy in form of heat.

Evaporation of water and PVP solutions at different temperatures were analyzed. Comparison of cross sectional areas over time revealed the expected behavior: the higher the temperature the faster the evaporation. In Figure 2 the cross sectional areas of water droplets are plotted against time at room temperature, 90 °C and 140 °C. In accordance with the d^2-law a linear correlation exists between the decrease of the squared radius r and time

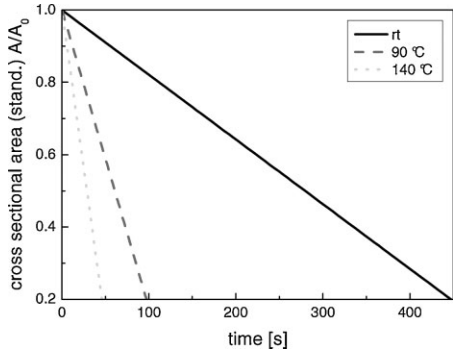

Figure 2.
Comparison of the standardized cross sectional area of water droplets at different temperatures.

t (Eq. (4)).[7] The influence of the ALF on the progress of the drying is negligible.

$$r^2 = r_0^2 - \beta t \text{ with}$$
$$\beta = \frac{2D_{10}M}{\rho_1 R}\left(\frac{p^*}{T_{ph}} - \frac{p_\infty}{T_\infty}\right)\frac{Sh}{2} \quad (4)$$

The diffusivity D_{10} of vapor in the gas phase, molecular mass M, liquid density ρ_1, saturation vapor pressure on the surface (p^*) and vapor pressure in the gas phase (p_∞) as well as temperatures on the surface (T_{ph}) and in the gas phase (T_∞) are combined in variable β describing the drying rate (unit m^2/s). The last term including the Sherwood number Sh accounts for forced convection around the droplet.[8]

Influence of the PVP Concentration on Drying Kinetics

If the drying process of solutions is investigated the influence of solid matter in the solvent on phase transition has to be regarded. Raoult's law correlates the vapor pressure p_L above a solution of a component B in solvent A with mole fraction x_A and vapor pressure p_A of the pure solvent (Eq. (5)).

$$p_L = p_A x_A + p_B x_B \quad (5)$$

At constant temperature a higher concentration of dissolved component B results in a decrease of the vapor pressure of solvent A. On the other hand polymer molecules will be arranged preferably at the surface of the droplet. This entropic effect results from gaining degrees of freedom when one polymer molecule displaces more than one solvent molecule. While every solvent molecule which moves into the bulk of the droplet gains a degree of freedom only one polymer molecule loses one degree of freedom. By replacing solvent molecules by polymer molecules the surface tension γ of the solution will be altered which in turn results in a changed phase transition rate.

For this reason the drying behavior of aqueous PVP solutions with different concentrations was investigated and compared to the evaporation of water (Figure 3). The decrease of the cross sectional area of PVP solutions proceeded faster than that of water. Even for a mass fraction of 5 wt% PVP the decrease was considerably higher and no further change in the decrease could be observed for higher concentrations of PVP.

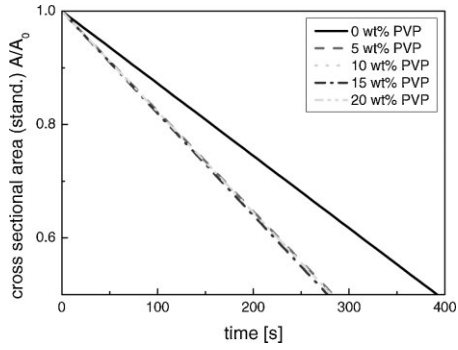

Figure 3.
Cross sectional area of water and aqueous PVP solutions with different concentrations.

The experiments disagree with the expected boiling-point elevation. A possible reason is the reduction of the surface tension by addition of polymer. The experiments displayed a higher mass transportation from the liquid into the gaseous phase if polymer was dissolved. Identical drying rates for mass fractions of 5 wt% and higher could be the result of a critical micelle concentration (CMC) where any further addition of polymer will increase the number of micelles but not the number of polymer molecules on the surface.

Influence of the Gas Flow on Drying Kinetics

During the falling period the evaporated solvent is constantly removed from the vicinity of the droplet. Mass and heat flow are enhanced by convection and proceed faster in comparison to a resting droplet. By increasing the droplet size the falling velocity of the droplet rises and the phase transition of the solvent into the gaseous phase occurs faster. The reason for this is that evaporated solvent will be removed more rapidly from the immediate vicinity

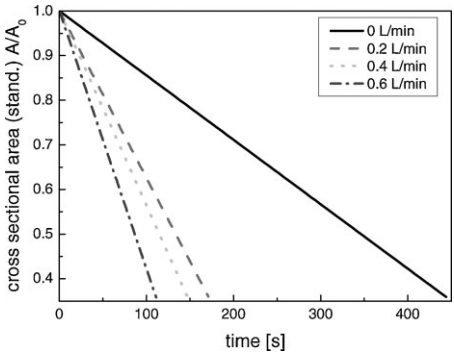

Figure 4.
Cross sectional areas of water droplets at room temperature with different gas flow velocities.

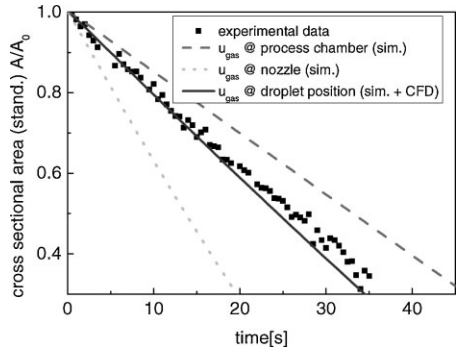

Figure 5.
Comparison of experimental data with numerical results for the drying of a 5 wt% PVP solution.

and the concentration gradient will be increased. In an acoustic levitator the relative velocity of the falling droplet can be simulated by generating a gas flow around the droplet.

To investigate the influence of the gas flow on the drying kinetics, experiments with water and aqueous PVP solutions were conducted. As expected the evaporation of the liquid proceeded faster with increasing gas flow for water as well as PVP solutions (Figure 4).

A numerical model to describe the drying kinetics of droplets of solid matter solutions which show negligible interaction with the solvent was developed and the results were compared to the experimental data. For a given gas flow only a range of drying rates could be determined, because the actual gas velocity at the position of the droplet was unknown. After exiting the gas nozzle in the reflector the gas flow rapidly expanded and the gas velocity decreased. Figure 5 displays limit cases where the upper limit represents the gas velocity in the nozzle and the lower one the velocity inside the whole process chamber.

Computational fluid dynamics (CFD) were used to determine the actual gas velocity at the position of the droplet. For a gas velocity of 1.9 m/s at the gas nozzle an actual velocity of 0.24 m/s at a distance of 12.3 mm between droplet and gas nozzle was simulated. The bulk of the gas flow thus did not reach the droplet but was distracted by flows to openings in the process chamber. Drying kinetics of the model were in good accordance with the experimental data when applying gas velocities simulated with CFD (Figure 5).

Comparison of PVP Morphologies Dried in an Acoustic Levitator and in a Spray Tower

An indicator for comparable conditions in levitator and spray tower is the obtained morphology of the dried particles. The formation of surface structures depends i.a. on temperature and solvent. If the temperature is below the solvents boiling point the evaporation occurs on the surface of the drying particles. For polymer solutions which yield particles with a smooth surface drying under these conditions results in hollow particles. Evaporation of solvent occurs on the surface and mass flow of solvent from the inside of the particle proceeds rapidly compared to the evaporation process. In the course of drying an indention forms on top and the surface bends inward until it reaches the bottom where either a fracture in the bottom surface produces a donut-like structure or if no rupture occurs a hollow particle with an opening on top forms.

For temperatures above the boiling point the evaporation proceeds faster than diffusion of solvent through the surface of the drying particle. The evaporation takes

place on the inside of the particle and inflates the particle. If there is only a small amount of solvent inside the particle it stays inflated and expanded hollow particles are obtained. If the volume of the evaporated solvent is considerably larger than the volume of the particle the surface bursts and collapses to gain a shriveled structure.

Drying of aqueous PVP solutions at different temperatures in the acoustic levitator yielded smooth surfaces at room temperature and partially shriveled structures at 60 °C and 90 °C. Partially shriveled structures could be the result of areas on the surface where cavities were formed and the shell collapsed on release of the water. For temperatures above the boiling point of water, i.e. at 140 °C, inflated as well as collapsed structures were obtained (Figure 6). Comparison with particles dried in a spray tower provided good conformance of morphology (Figure 6, bottom right).

Meshfree Simulation of Single Droplet Drying

Simulation of Morphology Evolution

The particle morphologies presented above cannot be described with common mathematical models for single droplet drying. These models commonly assume a spherically symmetric distribution of the relevant quantities (concentrations, temperature) over the entire droplet. Therefore only radial gradients are considered. Structures of higher dimensions can only be regarded using effective parameters, e.g. for transport inside a porous shell. A description of more complicated morphologies – like the ones presented above – will only be possible using a fully three-dimensional model.

Simulation of voidages, fractures, multiphase systems and moving interfaces inside a droplet is very challenging. Grid-based simulation methods suffer from the costly computation of the interface as well as the permanent grid adaptation. Further problems arise when large deformations need to be calculated. Meshfree methods offer a different approach based on a Lagrangian point of view. Calculation nodes are irregularly distributed over the domain and can – according to the laws of hydrodynamics – move independently without the need of remeshing. Particle-based methods, such as SPH, can address multiphase problems by using several kinds of particles with different behaviour for each phase. Movement and distortion of inter-

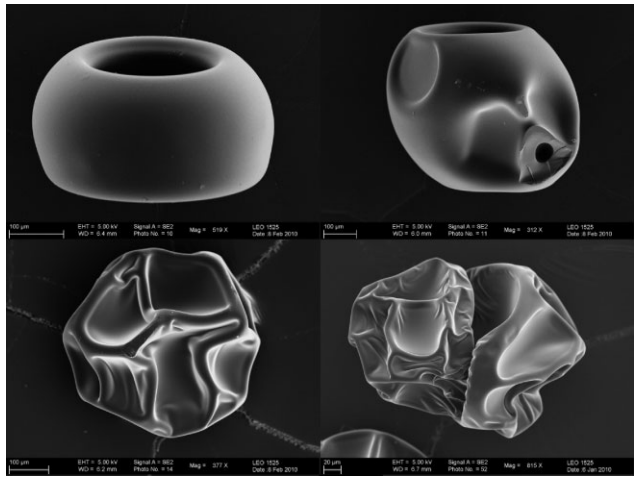

Figure 6.
Morphologies of particles dried in an acoustic levitator at room temperature (top left), 90 °C (top right), 140 °C (bottom left) as well as particles dried in a spray tower at a temperature ranging from 225 °C to 90 °C (bottom right).

faces can be followed by tracking interfacial particles.

Based on the method Smoothed Particle Hydrodynamics (SPH) a three-dimensional model is under development aiming on a detailed description of morphology evolution in a droplet. First results for the drying of a pure liquid droplet have been obtained. In future the model shall be enhanced to be capable of treating irregular morphologies like the ones originating from the experiments described above.

Smoothed Particle Hydrodynamics

The meshfree method Smoothed Particle Hydrodynamics was originally developed for astrophysical problems in 1977 by Lucy[9] and Gingold and Monaghan.[10] In SPH particles (interpolation points) represent a finite mass inside the whole simulation domain. Each particle bears a vector of inner variables such as temperature, concentrations etc., which represent the respective property for this part of the domain.

For a particle i a quantity f is represented in SPH using an integral approximation

$$f_i = \sum_j \frac{m_j}{\rho_j} f_j W_{ij}(h) \tag{6}$$

where m_j and ρ_j are mass and density of particle j. W is the smoothing kernel with a length scale (smoothing length) h. Theoretically every particle i interacts with all other particles and i itself. As the kernel has compact support and becomes zero for larger distances between i and j, only particles inside a certain radius from i need to be regarded.

The first spatial derivative of f can be evaluated using

$$\nabla f_i = \sum_j \frac{m_j}{\rho_j} f_j \nabla W_{ij}(h) \tag{7}$$

with the spatial derivative of the kernel W with respect to the distance r being

$$\nabla W_{ij}(h) = \mathbf{e_{ij}} \frac{dW_{ij}(h)}{dr} \tag{8}$$

where $\mathbf{e_{ij}}$ is the unit vector between particles i and j.[11] The second derivative is usually computed via

$$\left(\nabla^2 f\right)_i = 2 \sum_j \frac{m_j}{\rho_j} \frac{(f_i - f_j)}{|\mathbf{r_i} - \mathbf{r_j}|} \frac{dW_{ij}(h)}{dr} \tag{9}$$

Typical kernels amongst others are spline kernels. A continuum equation can be transformed into an SPH formulation by replacing the respective quantities or their derivatives by one of the summation formulas given above. Therefore model equations can be derived in a consistent way from continuum laws without additional parameterisation.

Model Equations

As SPH has been hardly used in chemical process engineering so far, an SPH model describing the drying of droplets had to be developed from scratch and validated in comparison to existing grid-based approaches. Hence in a first step simple equations for a spherically model were taken from Sloth et al[12] and then translated into an SPH formulation. For simplicity only a pure, single-phase liquid inside the droplet was considered.

The SPH model is written in Cartesian coordinates, as it shall be able to cope with non-spherical geometries later on. The SPH formulation for heat conduction inside the liquid droplet is expressed via[13]

$$c_{p,i} \frac{dT_i}{dt} = \sum_j \frac{m_j}{\rho_i \rho_j} \frac{4\lambda_i \lambda_j}{\lambda_i + \lambda_j} \frac{T_i - T_j}{|\mathbf{r_i} - \mathbf{r_j}|} \frac{dW_{ij}(h)}{dr} \tag{10}$$

where t is time, T the temperature, c_p the specific heat capacity and λ the heat conduction of the liquid. The vector $\mathbf{r}$ represents the position of a particle.

Heat and mass fluxes calculated by Nusselt and Sherwood correlations cannot be implemented directly in SPH as the heat transfer coefficient α and the mass transfer coefficient β are area-based parameters and SPH particles are volume based. Using the CSF model originally developed for the calculation of surface tension by Brackbill et al[14] the area to volume fraction can be

found via the following expression:

$$\frac{\nabla c}{[c]} = \frac{1}{[c]} \sum_j V_j c_j \nabla W_{ij}(h) \tag{11}$$

V is the particle volume and c a colour function, which has different values on both sides of the interface and therefore can be used for interface detection. Here the particle type is used as a colour function. The gradient of the colour function divided by its jump across the interface [c] yields the relation of area to volume for an interface particle. Details can be found in[15] and.[16]

The mass transfer across the interface for a liquid boundary particle i is modelled by

$$\frac{dm_i}{dt} = -2V_i MW_l \frac{\nabla c}{[c]} \frac{\beta}{\Re T}(p_{v,i} - p_{v,\infty}) \tag{12}$$

MW_l is the molar weight of the liquid, β the mass transfer coefficient and R the ideal gas constant. The vapour pressure p_v is calculated using Antoine's law for the temperatures at the droplet surface and far away from the droplet (T_∞) respectively.

The heat transfer across the interface particle is added as a source term to Eq. (10) for interfacial fluid particles

$$c_p \frac{dT_i}{dt} = \sum_j \frac{m_j}{\rho_i \rho_j} \frac{4\lambda_i \lambda_j}{\lambda_i + \lambda_j} \frac{T_i - T_j}{|\mathbf{r_i} - \mathbf{r_j}|} \frac{dW_{ij}(h)}{dr} - 2\frac{\nabla c}{[c]} \frac{\alpha}{\rho}(T_i - T_\infty) \tag{13}$$

where α is the heat transfer coefficient. The temperature change due to the latent heat of vaporisation is also added to the respective particles.

Gas particles are kept at a distinct temperature (T_∞) and vapour pressure and particle positions are kept constant. Timesteps are computed using explicit time integration. The mass of a liquid, interfacial particle decreases until it reaches zero. Then the particle will be transformed into a gas particle.

Results

Calculations have been performed for a droplet of radius 0.3 mm. For simplicity the particles were adjusted in a cubic alignment. All particles are of the same size. Figure 7 shows an example setup consisting of 1300 particles with dots representing liquid particles and circles standing for gas particles. Only a part of the whole droplet was calculated to keep the computational effort reasonable.

Figure 8 shows results of the SPH model in comparison to a mesh-based calculation for a droplet (left) and a flat geometry (right). It can be seen that the SPH approach matches the mesh-based results very well, regardless of the surface curvature. This is a very important point for simulations of morphology evolution as interfaces will be arbitrarily shaped.

Modelling Morphology Evolution Using SPH

Meshfree approaches have been proven to be applicable to structure forming processes.[17] However methods like DEM represent material behaviour such as a visco-plastic one by spring-damper systems.

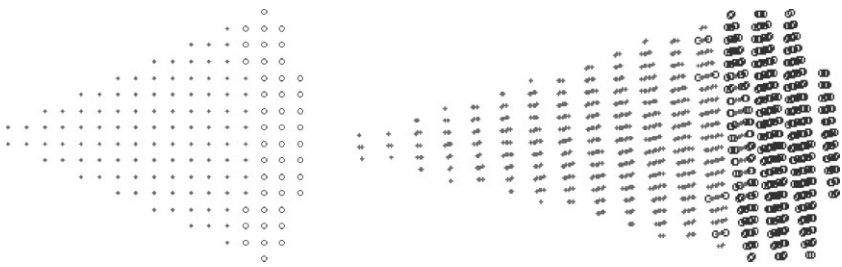

Figure 7.
Particle setup with 1300 particles, 2D projection (left), full 3D setup (right).

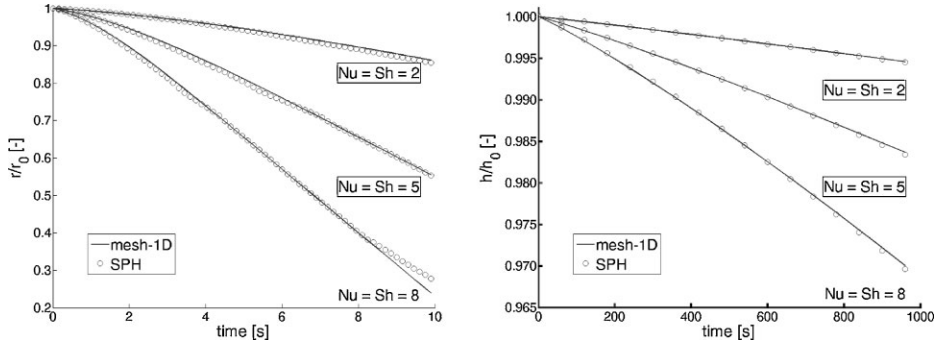

Figure 8.
Drying of a droplet (left, $r_o = 0.3$ mm) and an infinitely extended water bassin (right, $h_o = 0.1$ m) with initial $T_l = 50\,^{\circ}C$ and outer conditions $T_g = 60\,^{\circ}C$, $rH = 50\%$.

The parameterisation of these particle-particle interactions strongly affects the simulation result and cannot be derived directly from continuum laws. A consistent derivation of model equations from continuum laws as in SPH is desirable.

To show the capability of the SPH approach to model morphology determining processes a simple two-dimensional example of a structure-forming process determined by different material behaviour is presented in the next paragraph. Details can be found in.[18]

Figure 9, frame 1 shows the computational domain. Different particle colours signify different materials and material behaviour. Grey particles are polymer with a visco-plastic Bingham behaviour described by the Cross model.[19] The black-white particles in rhomb shape in the middle represent a visco-plastic wax. A solid is modelled as a linear elastic material represented with black particles.

The viscoplastic wax decomposes together with oxygen diffusing from the upper boundary. A pore consisting of a gaseous blowing agent is formed (frames 2-3). When the pressure inside the pore exceeds the polymer yield stress, the polymer begins to flow (frames 4-5).

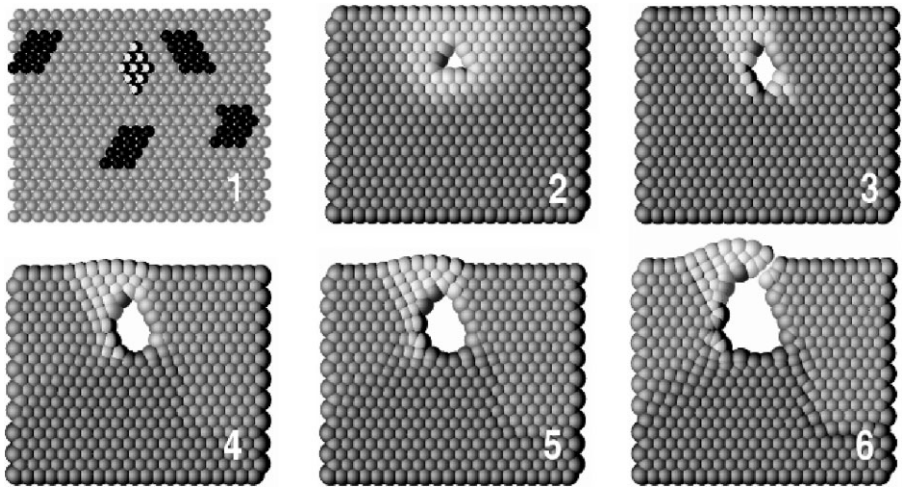

Figure 9.
SPH simulation of the development of a single pore in a visco-plastic substrate.

Due to the irregularly distributed solids the deformation is not symmetric. When the polymer cracks, pressure compensation with the surrounding takes place and the polymer deformation stops. The final porous structure is shown in frame 6.

Conclusion

Acoustic levitation was investigated as an adequate model for spray processes regarding drying kinetics and morphology formation. Drying of aqueous PVP solutions demonstrated reproducibility and displayed good accordance of morphology for particles dried in an acoustic levitator and in a spray tower. The influence of PVP in aqueous solutions on the drying kinetics disagreed with Raoult's law (Eq. (5)). Further studies regarding the surface tension of PVP solutions and concentration of dissolved polymer in water have to be conducted. All things considered the experiments confirmed acoustic levitation as a comparably inexpensive technology that allows for fast and simple insights into spray processes.

Meshfree simulations have proven to be capable of modelling morphology determining processes. Multiphase systems with moving interfaces and strong distortions can be represented. A new droplet drying model based on an SPH approach has been developed and validated. More advanced studies regarding droplet drying and polymerisation based on this approach will be developed in future and experimentally validated with experiments in an acoustic levitator.

Acknowledgements: This collaboration is part of the DFG research program ''Prozess Spray''. The authors kindly thank the Deutsche Forschungsgemeinschaft for the financial support.

[1] W. Rähse, O. Dicoi, *Chem. Ing. Tech.* **2009**, *81*, 699–716.
[2] L. V. King, *Proc. R. Soc. London, Ser. A* **1934**, *147*, 212–240.
[3] E. H. Trinh, *Rev. Sci. Instrum.* **1985**, *56*, 2059–2065.
[4] E. G. Lierke, *Act. Acust. United Ac.* **2002**, *88*, 206–217.
[5] E. G. Lierke, *Acta Acust.* **1996**, *82*, 220–237.
[6] R. Tuckermann, S. Bauerecker, B. Neidhart, *Phys. Unserer Zeit* **2001**, *32*, 69–75.
[7] M. Peglow, T. Metzger, G. Lee, H. Schiffter, R. Hampel, S. Heinrich, E. Tsotsas, in: ''*Modern Drying Technology, Volume 2 – Experimental Techniques*'', E., Tsotsas, A. S. Mujumdar, Eds., Wiley-VCH, Weinheim 2009, p. 56.
[8] R. Tuckermann, S. Bauerecker, B. Neidhart, *Anal. Bioanal. Chem.* **2002**, *372*, 122–127.
[9] L. B. Lucy, *Astron. J.* **1977**, *82*, 1013–1024.
[10] R. A. Gingold, J. J. Monaghan, *Mon. Not. Roy. Astron. Soc.* **1977**, *181*, 375–389.
[11] S. Rosswog, *New Astron. Rev.* **2009**, *53*, 78–104.
[12] J. Sloth, S. Kiil, A. D. Jensen, S. K. Andersen, K. Jørgensen, H. Schiffter, G. Lee, *Chem. Eng. Sci.* **2006**, *61*, 2701–2709.
[13] J. J. Monaghan, *Rep. Prog. Phys.* **2005**, *68*, 1703–1759.
[14] J. U. Brackbill, D. B. Kothe, C. Zemach, *J. Comput. Phys.* **1992**, *100*, 335–354.
[15] W. Säckel, F. Keller, U. Nieken, in: ''Proceedings of IDS 2010'', forthcoming, Magdeburg, October 3rd – 6th **2010**.
[16] W. Säckel, F. Keller, U. Nieken, in: ''*Proceedings of SPRAY 2010*'', U., Fritsching, E. Gutheil, Eds., Heidelberg May 3rd – 5th 2010.
[17] B. Ledvinkova, F. Keller, J. Kosek, U. Nieken, *Chem. Eng. J.* **2008**, *140*, pp. 578–585.
[18] F. Keller, U. Nieken, in: ''*Proceedings of Meshfree Methods for Partial Differential Equations V*'', forthcoming 2010, M., Griebel, M. A. Schweitzer, Eds., Bonn August 17th – 19th 2009.
[19] R. J. Young, P. A. Lovell, ''*Introduction to Polymers*'', 2nd edition, Chapman & Hall, London 1995.

